Received 14 March 2019; revised 9 July 2019 and 13 August 2019; accepted 1 September 2019. Date of publication 4 September 2019; date of current version 30 September 2019. The review of this article was arranged by Editor K. Shenai.

Digital Object Identifier 10.1109/JEDS.2019.2939223

A Snapback-Free and Low Turn-Off Loss Reverse-Conducting SOI-LIGBT With Embedded Diode and MOSFET

JIAYU WU, HAIMENG HUANG (Member, IEEE), BO YI (Member, IEEE), HAO HU, HUAN HU, AND XING BI CHEN (Fellow, IEEE)

State Key Laboratory of Electronic Thin Films and Integrated Devices, University of Electronic Science and Technology of China, Chengdu 610054, China

CORRESPONDING AUTHOR: X. B. CHEN (e-mail: xbchen@uestc.edu.cn)

This work was supported in part by the National Science Foundation of China for Young Scholars under Grant 61804021, and in part by the Open Foundation of State Key Laboratory of Electronic Thin Films and Integrated Devices under Grant KFJJ201708.

ABSTRACT A novel snapback-free and low turn-off loss reverse-conducting (RC) SOI-LIGBT is proposed and investigated by numerical simulations. An n-MOSFET (M_{N2}) is embedded in the anode side of the LIGBT to short the P-anode/N-buffer junction during the turn-off transient, thus allowing the LIGBT to be turned off rapidly without excessive tail current. In addition, M_{N2} enable the LIGBT to conduct the reverse conducting current like the freewheeling diode. In the forward-conducting state, M_{N2} is turned off, then the proposed LIGBT operates like a conventional one and the snap-back is avoided. The gate electrode of M_{N2} can be controlled synchronously by the gate signal of the LIGBT which is level-shifted by a p-i-n diode (D_1) and processed by an anode-controlling circuit, and therefore, the proposed RC-LIGBT still maintains a three-terminal configuration. D_1 and M_{N2} are embedded in the drift region and anode-side of the LIGBT, respectively, and they can be isolated by deep-oxide trenches. The numerical simulation results reveal that the turn-off loss (E_{off}) and reverse recovery charge of the proposed LIGBT is reduced by 58.3% and 38.9%, respectively, compared with the conventional LIGBT combining with antiparallel freewheeling diode.

INDEX TERMS RC-LIGBT, snapback-free, turn-off loss, reverse recovery charge.

I. INTRODUCTION

The lateral insulated gate bipolar transistor (LIGBT) on silicon-on-insulator (SOI) has been widely used in the medium voltage range of smart power integrated circuits [1], [2]. As a unidirectional device, the conventional LIGBT needs an antiparallel diode in various power applications to conduct reverse current, which induces extra cost and parasitic effects [3]. The shorted-anode LIGBT implements reverse-conducting by introducing an N^+ region in the anode side of the LIGBT, which undesirably leads to the snap-back effect in the forward-conducting state [4], [5]. Some methods have been reported to suppress the snap-back problem [6]–[9] by increasing the resistor for the electron current from the N^+ anode to the P^+ anode, which causes a higher on-state voltage drop (V_{on}) compared with that of the conventional LIGBT. Dual-gate devices [10]–[13] also have been reported to be able to eliminate the snap-back effect and improve the turn-off speed, nevertheless, these devices require extra control circuits or high voltage devices to switch the anode-gate.

In this paper, we propose a novel RC-LIGBT with embedded p-i-n diode (D_1) and n-MOS transistor (M_{N2}). The gate signal of the LIGBT which is level-shifted by D_1 and processed by an anode-controlling circuit can synchronously control M_{N2} to short the anode junction of the LIGBT during the turn-off transient and the reverse-conducting state. Thus, the LIGBT is a three-terminal device without extra controlling signal. The snap-back phenomenon is eliminated in forward-conducting state. The turn-off loss and reverse recovery charge are reduced. The electrical characteristics

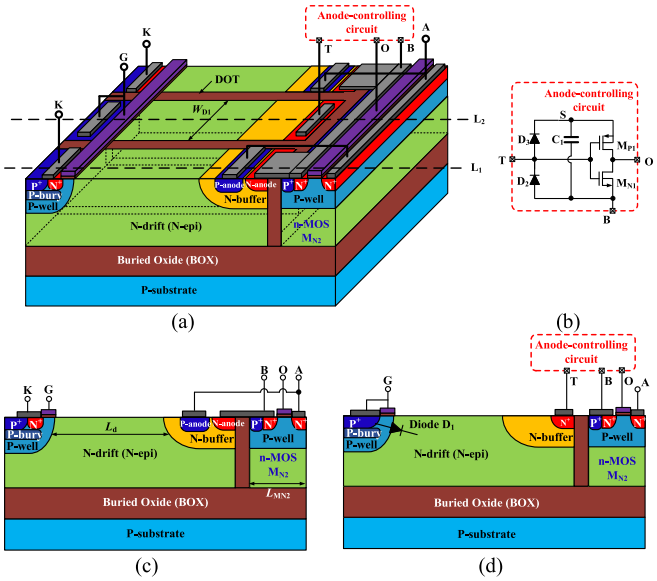

FIGURE 1. **(a) 3-D cell view of the proposed LIGBT with (b) the block diagram of the anode-controlling circuit. Cross sections of the proposed structure along the line L_1 (c) and L_2 (d).**

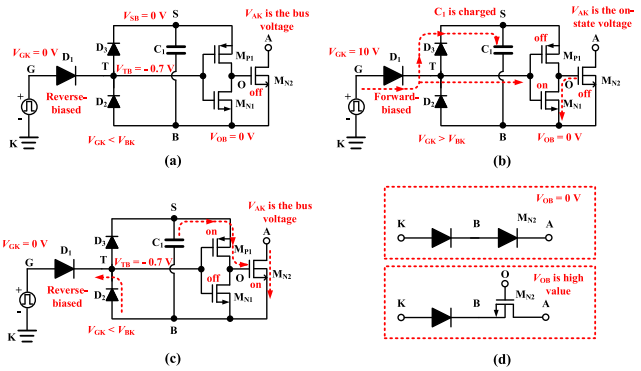

FIGURE 2. **Operation of the proposed RC-LIGBT during (a) the power-on process, (b) the forward-conducting state, (c) the turn-off process, and (d) the reverse-conducting state.**

of the proposed RC-LIGBT are investigated by Sentaurus TCAD tools.

II. DEVICE STRUCTURE AND MECHANISM

Fig. 1(a) shows the 3-D cell view of the proposed RC-LIGBT. The inside and outside part of the proposed structure are all active LIGBT region, and the middle part isolated by deep-oxide trench is D_1, which has the same breakdown voltage (BV) as the LIGBT region. Its width (W_{D1}) is 10 μm. On the right side of the cell, M_{N2} is formed and also isolated by the deep-oxide trench. The drain electrode and source electrode of M_{N2} are connected to the P-anode and N-anode of the LIGBT, named as electrodes A and B, respectively. The gate electrode of M_{N2} is connected to the output terminal (O) of the anode-controlling circuit. The input terminal (T) of the anode-controlling circuit is connected to the N^+ cathode of D_1. The P^+ anode of D_1 is connected to the gate electrode (G) of the LIGBT. The anode-controlling circuit, as depicted in Fig. 1(b), consists of two low-voltage diodes (D_2 and D_3), a power supply capacitor (C_1) and a CMOS inverter (consists of M_{P1} and M_{N1}), which can be integrated on the right side of M_{N2}. The contact B serves as the reference ground of the anode-controlling circuit. Table 1 lists the key design parameters for the proposed structure and the anode-controlling circuit. A conventional LIGBT and a freewheeling diode with the same parameters are also designed for comparison. The operation principle of the proposed RC-LIGBT with the anode-controlling circuit will be described later.

A. POWER-ON PROCESS OF THE PROPOSED RC-LIGBT

As shown in Fig. 2(a), during the power-on process, V_{GK} = 0 V, V_{AK} and V_{BK} rise to the bus voltage. The diodes D_2 is forward biased. D_1 and D_3 are reverse biased to make $V_{TB} = -0.7$ V. Since the LIGBT has not been turned on before, C_1 is not charged and V_{SB} (the voltage across C_1) is 0 V. The output of the CMOS inverter (V_{OB}) is 0 V and M_{N2} is in OFF-state.

B. FORWARD-CONDUCTING STATE OF THE PROPOSED RC-LIGBT

As depicted in Fig. 2(b), during the forward-conducting state, $V_{GK} = 10$ V, and V_{BK} is close to the ON-state voltage drop of the LIGBT ($V_{BK} < V_{GK} = 10$ V). Thus, D_1 and D_3 are forward biased, and D_2 is reverse biased to make V_{TB} rise from -0.7 V in the blocking state to a high value. C_1 is charged, M_{P1} is turned off and M_{N1} is turned on. V_{OB} keeps to 0 V, and then, M_{N2} is still off. Since the current path from the N-anode to the P-anode is blocked, the electron current can only flow through the P-anode, thus the proposed LIGBT can inject holes into the drift region like the conventional one without snap-back phenomenon.

C. TURN-OFF PROCESS OF THE PROPOSED LIGBT

When V_{GK} drops from 10 V to 0 V, both V_{AK} and V_{BK} will rise as the LIGBT is turned off ($V_{BK} > V_{GK}$). Hence, D_2 is forward biased, D_1 and D_3 are reverse biased to make V_{TB} drops from high value to -0.7 V. V_{SB} maintains high value attributed to the fact that the voltage drop of the capacitor C_1 cannot be abruptly changed, and accordingly, M_{P1} is turned on and M_{N1} is turned off, V_{OB} increases from 0 V to the value of V_{SB}. Consequently, M_{N2} is turned on, and the P-anode/N-buffer junction is shorted to prevent the injection of holes and thereby the long tail current is eliminated. After the LIGBT is turned off and in the blocking state, M_{N2} will remain in the ON-state because $V_{TB} = -0.7$ V and C_1 has been charged until the LIGBT is turned on.

D. REVERSE-CONDUCTING STATE OF THE PROPOSED LIGBT

Fig. 2(d) reveals the equivalent circuit diagram of the proposed LIGBT when it is in the reverse-conduction state.

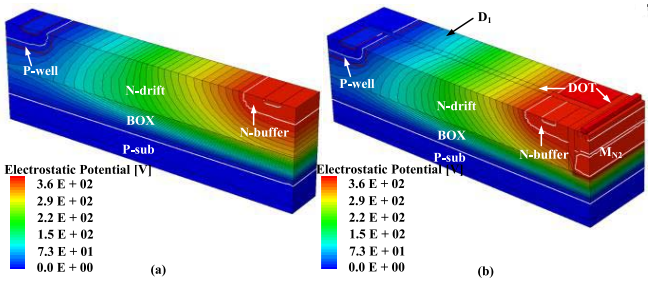

FIGURE 3. Potential contours of (a) the conventional LIGBT and (b) the proposed LIGBT at BV of 363 V and 362 V, respectively (10V/contour).

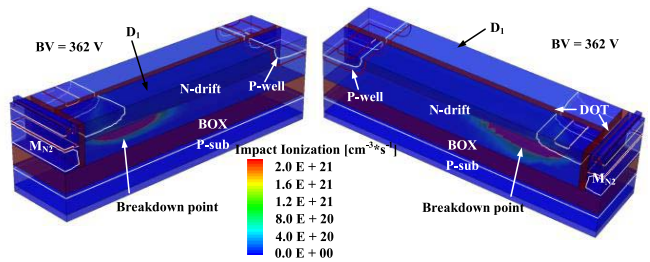

FIGURE 4. The total generation rate due to impact ionization of the proposed structure.

If the LIGBT is not turned on before, it is known from the previous discussion that M_{N2} is in the OFF-state. Hence, the reverse-conducting current through M_{N2} is mainly the body diode current. Then,the whole current path from electrode K to A consists of two diode in series. If the LIGBT has been turned on before, M_{N2} is in the ON-state, and the reverse-conducting current through M_{N2} is mainly the channel current. Consequently, the whole current path from electrode K to A consists of one diode and one n-MOSFET in series. In both cases, the reverse-conduction of the LIGBT can be implemented.

III. SIMULATION RESULTS AND ANALYSIS

The behaviors of the new device is investigated by 3-D numerical simulations. Since the proposed structure is symmetrical, half of its cell are used for simulation to reduce the number of grid points. Fig. 3 depicts the potential contours of the proposed LIGBT and the conventional one at BV of 362 V and 363 V, respectively (10 V/contour). The BV of the proposed structure is not significantly reduced in comparison with that of the conventional one. Fig. 4 exhibits the total generation rate of the proposed structure due to impact ionization. It can be seen that the breakdown point of the device locates at the bottom of the SOI layer, and there is no significant difference from that of other SOI lateral devices.

Fig. 5 depicts the conduction characteristics of the LIGBTs. The SSA LIGBT [6] is designed with the same parameters in Table 1 for comparison and the length between N^+ anode to the N-buffer region (L_S) is set as 20 μm to suppress the snap-back effect. The width (z-dimensions) ratio of the conventional LIGBT to the conventional antiparallel

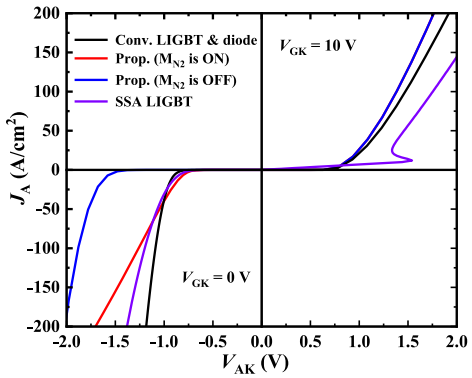

FIGURE 5. Conduction characteristics of the LIGBTs with V_{GK} = 10 V and 0 V.

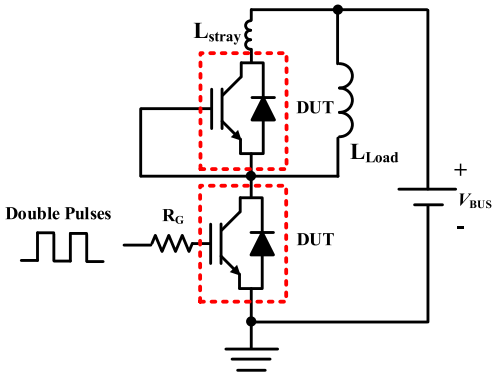

FIGURE 6. Mixed-mode inductive switching circuit with V_{BUS} = 150 V, L_{Load} = 1.5 mH, L_{stray} = 10 nH, and R_G = 10 Ω.

freewheeling diode is 4:1, and the total area is considered for calculating the current density. For the proposed structure, the width ratio of the active LIGBT region to the M_{N2} is also 4:1 and the total area is considered for calculating the current density. As shown in Fig. 5, in the forward-conducting state, the proposed structure is snapback-free since M_{N2} is in OFF-state. Meanwhile, the current density of the proposed structure is higher than other structures when the total area is considered for calculating the current density. In the reverse-conducting state, the knee voltages of the proposed structure with M_{N2} in OFF-state and in ON-state are 1.4 V and 0.7 V, respectively.

The mixed-mode inductive switching circuit shown in Fig. 6 is utilized to simulate the turn-off and reverse recovery characteristics. All of the three devices are turned off under the current of 1 A (J = 100 A/cm^2). The area of the proposed structure and the SSA LIGBT are all set as 1 mm^2. And the total area of the conventional LIGBT combining with the conventional antiparallel freewheeling diode is set as 1 mm^2 for comparison. The lifetimes of the electrons and the holes are both set as 1 μs.

Fig. 7 reveals the transient waveforms of V_{GK} and V_{OB} (the gate voltage of M_{N2}) during the switching process of the proposed LIGBT. When the LIGBT is in the turn-off process, V_{GK} jumps from high level to low level and V_{OB}

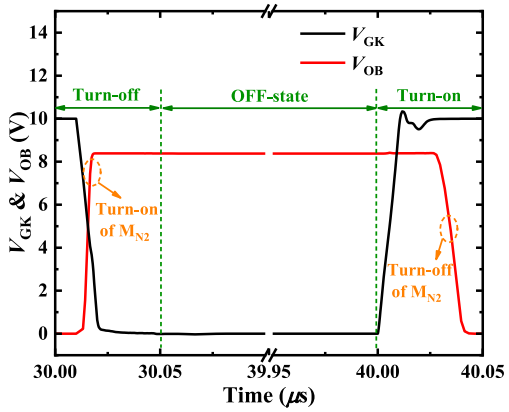

FIGURE 7. Transient waveforms of V_{GK} and V_{OB} during the switching process.

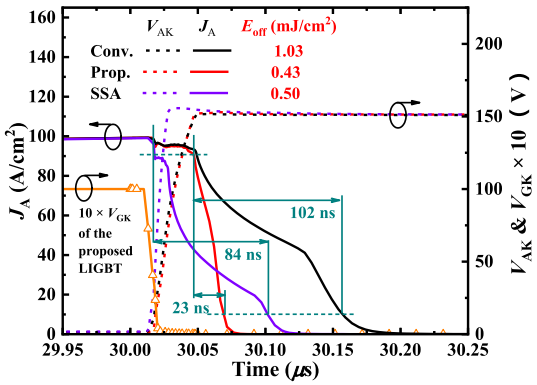

FIGURE 8. Turn-off characteristics of the three LIGBTs.

increases to high level almost simultaneously. Then, M_{N2} is turned on and the P-anode/N-buffer junction of the LIGBT is shorted. When the LIGBT is in the turn-on process, V_{GK} jumps from low level to high level and V_{OB} decreases to 0 V. Then, M_{N2} is turned off and the holes can be injected to the N-drift region from the P-anode with no snap-back effect.

The turn-off characteristics of the three LIGBTs are illustrated in Fig. 8. The proposed device exhibits the shorter fall time of tail-current and the lower turn-off loss (E_{off}) than the other two LIGBTs. The E_{off} of the proposed device decreases by 58.3% at V_{on} = 1.38 V, compared with the conventional LIGBT.

The reverse recovery characteristics of the proposed LIGBT, the SSA LIGBT and the antiparallel freewheeling diode are demonstrated in Fig. 9. The reverse recovery charge (Q_{rr}) of the proposed LIGBT with M_{N2} in ON-state are less than that of the freewheeling diode by 38.9%. The reverse recovery charge and time of the proposed device with M_{N2} in OFF-state are larger and longer than that of the proposed device with M_{N2} in ON-state. This is because that during the reverse recovery process of the device with M_{N2} in OFF-state, more electrons are injected into P-anode which causes more holes to be injected into the N-drift region.

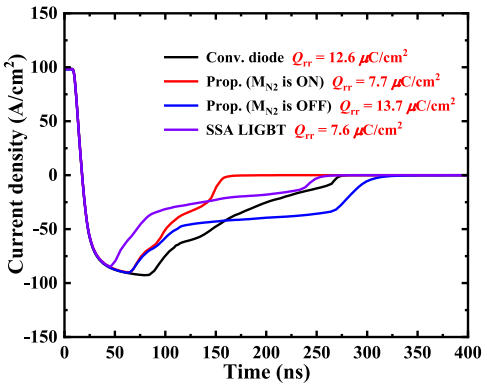

FIGURE 9. Reverse recovery characteristics of the proposed LIGBT, the SSA LIGBT and the conventional diode.

TABLE 1. Key design parameters.

Structure Parameters	Values
BOX thickness (μm)	3
N-drift thickness (μm)	6
N-drift length, L_d (μm)	27
N-drift concentration (cm^{-3})	2×10^{15}
P-well concentration (cm^{-3})	2×10^{17}
P-bury concentration (cm^{-3})	3×10^{18}
N-buffer concentration (cm^{-3})	2×10^{17}
P-anode concentration (cm^{-3})	1×10^{18}
N-anode concentration (cm^{-3})	1×10^{20}
Gate oxide thickness (nm)	50
Width of deep-oxide trenches (μm)	1
Width of the diode D_1, W_{D1} (μm)	10
Length of the M_{N2}, L_{MN2} (μm)	3
The value of capacitor C_1 (pF)	100
The W/L of M_{P1} (μm)	200 / 1
The W/L of M_{N1} (μm)	100 / 1
The breakdown voltage of D_2 and D_3	15 V

TABLE 2. Comparison of the characteristics among these devices.

@ J = 100 A/cm²		Conv. LIGBT & diode	SSA LIGBT	The proposed LIGBT	
				M_{N2} is ON	M_{N2} is OFF
FC-State	$V_{on\text{-}FC}$ (V)	1.47	1.75	-	1.38
	E_{off} (mJ/cm²)	1.03	0.50	0.43	-
	FOM1 = V_{on} ×E_{off}	1.514	0.875	0.593	
RC-State	$V_{on\text{-}RC}$ (V)	1.09	1.20	1.26	1.88
	Q_{rr} (μC/cm²)	12.6	7.6	7.7	13.7
	FOM2 = V_{on} ×Q_{rr}	13.734	9.12	9.702	25.756

Table 2 shows the comparison of the characteristics between the conventional LIGBT combining with freewheeling diode, the SSA LIGBT and the proposed LIGBT. In the forward-conducting state, the proposed structure exhibits superior tradeoff relationship between V_{on} and E_{off} and its figure of merit (FOM1 = $V_{on\text{-}FC} \times E_{off}$) is reduced

by 60.8% compared with the conventional LIGBT. In the reverse-conducting state, the FOM2 ($= V_{\text{on-RC}} \times Q_{\text{rr}}$) of the proposed structure with M_{N2} in ON-state reduced by 33.9% compared with the conventional antiparallel freewheeling diode. Although the FOM2 of the proposed structure with M_{N2} in OFF-state is relatively higher than other devices, in practical applications, once the LIGBT has been turned on and C_1 has been charged, M_{N2} will always maintain ON-state when the proposed structure is in the reverse-conducting state.

IV. CONCLUSION

3-D numerical simulation results demonstrate that the proposed RC-LIGBT has promising performances on the output characteristics, the turn-off loss, and the reverse recovery charge. And the fabrication process of the proposed structure is compatible with the existing SOI process [9], [14]. The proposed structure decreases the turn-off loss and reverse recovery charge by 58.3% and 38.9%, respectively, compared with the conventional LIGBT combining with antiparallel freewheeling diode.

REFERENCES

[1] W. Sun *et al.*, "A novel silicon-on-insulator lateral insulated-gate bipolar transistor with dual trenches for three-phase single chip inverter ICs," *IEEE Electron Device Lett.*, vol. 36, no. 7, pp. 693–695, Jul. 2015. doi: 10.1109/LED.2015.2434611.

[2] Q. Qian, S. Liu, W. Sun, H. Wang, and C. Zhang, "A robust W-shape-buffer LIGBT device with large current capability," *IEEE Trans. Power Electron.*, vol. 29, no. 9, pp. 4466–4469, Sep. 2014. doi: 10.1109/TPEL.2014.2299822.

[3] K. Hara *et al.*, "600V single chip inverter IC with new SOI technology," in *Proc. ISPSD*, 2014, pp. 418–421. doi: 10.1109/ISPSD.2014.6856065.

[4] P. A. Gough, M. R. Simpson, and V. Rumennik, "Fast switching lateral insulated gate transistor," in *Proc. IEDM*, 1986, pp. 218–221. doi: 10.1109/IEDM.1986.191153.

[5] M. R. Simpson, "Analysis of negative differential resistance in the I–V characteristics of shorted-anode LIGBT's," *IEEE Trans. Electron Devices*, vol. 38, no. 7, pp. 1633–1640, Jul. 1991. doi: 10.1109/16.85160.

[6] J.-H. Chul, D.-S. Byeon, J.-K. Oh, M.-K. Han, and Y.-I. Choi, "A fast-switching SOI SA-LIGBT without NDR region," in *Proc. ISPSD*, 2000, pp. 149–152. doi: 10.1109/ISPSD.2000.856793.

[7] J. Oh, D. H. Chun, R. Oh, and H. S. Kim, "A snap-back suppressed shorted-anode lateral trench insulated gate bipolar transistor (LTIGBT) with insulated trench collector," in *Proc. IEEE Int. Symp. Ind. Electron.*, Gdansk, Poland, 2011, pp. 1367–1370. doi: 10.1109/ISIE.2011.5984358.

[8] L. Huang *et al.*, "A snapback-free fast-switching SOI LIGBT with polysilicon regulative resistance and trench cathode," *IEEE Trans. Electron Devices*, vol. 64, no. 9, pp. 3961–3966, Sep. 2017. doi: 10.1109/TED.2017.2726080.

[9] L. Zhang *et al.*, "A high current density SOI-LIGBT with segmented trenches in the anode region for suppressing negative differential resistance regime," in *Proc. ISPSD*, Hong Kong, 2015, pp. 49–52. doi: 10.1109/ISPSD.2015.7123386.

[10] F. Udrea, U. N. K. Udugampola, T. Trajkovic, and G. A. J. Amaratunga, "Reverse conducting double gate lateral insulated gate bipolar transistor in SOI based technology," in *Proc. 19th Int. Symp. Power Semicond. Devices IC's*, Jeju, South Korea, 2007, pp. 221–224. doi: 10.1109/ISPSD.2007.4294972.

[11] B.-H. Lee *et al.*, "A new gradual hole injection dual-gate LIGBT," *IEEE Electron Device Lett.*, vol. 19, no. 12, pp. 490–492, Dec. 1998. doi: 10.1109/55.735756.

[12] K. Sheng *et al.*, "Dual gate lateral inversion layer emitter transistor," in *Proc. Int. Conf. Power Electron. Mach. Drives*, Jun. 2002, pp. 37–40.

[13] J. Wei *et al.*, "Ultrafast and low-turn-off loss lateral IEGT with a MOS-controlled shorted anode," *IEEE Trans. Electron Devices*, vol. 66, no. 1, pp. 533–538, Jan. 2019. doi: 10.1109/TED.2018.2873766.

[14] *X-FAB SOI Process Technologies*. Accessed: Feb. 15, 2019. [Online]. Available: https://www.xfab.com/technology/soi/